Macromolecules

COMMUNICATION TO THE EDITOR

pubs.acs.org/Macromolecules

On the Onset of Oriented Structures in Flow-Induced Crystallization of Polymers: A Comparison of Experimental Techniques

Michelle D'Haese,[†] Oleksandr O. Mykhaylyk,*[,‡] and Peter Van Puyvelde*[,†]

[†]Leuven Material Research Centre, Department of Chemical Engineering, Katholieke Universiteit Leuven, W. de Croylaan 46, B-3001 Leuven, Belgium

[‡]Department of Chemistry, University of Sheffield, Sheffield S3 7HF, United Kingdom

INTRODUCTION

During processing, polymers are subjected to complex thermomechanical histories during which the final morphology is formed. Nowadays, it is widely known that the applied flow field can drastically enhance polymer crystallization, mainly through an acceleration of the nucleation process.[1] In addition, under the appropriate conditions, the crystal morphology can be altered from spherulites to shish-kebab structures. Although already observed in the 1960s,[2] interest in this shish-kebab morphology is still present. The latter is due to the important mechanical properties that are attributed to such structures, but also to the underlying formation mechanism which is still not completely understood. Recently, however, the existence of threshold flow conditions for the onset of oriented morphologies has been identified.[3−6] This flow condition is set by a critical value of the mechanical work w that needs to be applied to the polymer melt at shear rates $\dot{\gamma}$ larger than the inverse of the Rouse time of the longest polymeric chains in the polymer ensemble. This mechanical work is calculated as[7]

$$w = \int_0^{t_s} \eta(\dot{\gamma}(t))\dot{\gamma}^2(t)\,\mathrm{d}t \qquad (1)$$

in which η is the shear rate dependent viscosity and the integration is performed over the entire time of shearing t_s. The latter observation is important since it identifies the parameters that are responsible for the formation of the oriented structures. It demonstrates that not only the shear rate is important in order to be able to stretch the longest chains but also the time of stretching needs to be sufficiently long in order to grow the resulting shish morphology. Different experimental methods have been proposed in literature to determine the "critical" value of the mechanical work that needs to be applied to the polymer.[3−6] In this Communication, two different experimental approaches will be compared. One method is based on a rectilinear flow field and online birefringence measurements whereas the other is based on torsional flow and offline small-angle X-ray scattering (SAXS). Samples originating from both geometries will be analyzed by one and the same method, SAXS, to be able to compare the techniques. In addition, the temperature dependence of the threshold flow condition will be investigated.

MATERIALS

In this work, isotactic poly(1-butene) PB-400, provided by Basell, has been used. It has an isotacticity of 98.8% and does not contain any nucleating agents. The molecular weight and polydispersity index are 176 kg/mol and 5.7, respectively. Under the conditions used in this work, the polymer crystallizes in the unstable polymorphic form II (melting point of spherulitic morphology 111 °C). It is known that after 10 days of aging at room temperature the tetragonal crystals of form II transform into more stable trigonal form I without changing their stacked lamellae structure and overall mass degree of crystallinity.[9] Thus, even if the structural morphology is not affected by the phase transition, it has to be noted that online measurements carried out in this work probe time scales much shorter than the time scale of the phase transition and hence deal mainly with the phase II and the amorphous component. Offline measurements, on the other hand, performed a few months later after the shear-induced crystallization, deal mainly with the stable phase I and the amorphous component.

METHODOLOGY

In this work, different flow geometries have been used to study flow-induced crystallization phenomena: rectilinear (or sliding) parallel plates and torsional disks (Figure 1). Whereas the former has the undoubtful advantage of producing a uniform shear rate across the sample, the latter has the advantage of probing different shear rates at the same time (see Figure 1).

Since the polymer sheared in the sliding plate geometry experiences the same flow conditions everywhere in the sample, only one point needs to be tracked in this setup to obtain information about shear-induced crystallization. This gives a wide range of opportunities to couple this geometry with online measurements including birefringence, which can effectively be used for time-resolved measurements of fast processes. Thus, in the first setup, the sliding plate geometry is combined with a commonly used online polarimetry setup that is able to detect the birefringence in an *in situ* and *time-resolved* manner.[8,10] The birefringence experiments were performed using an optical train consisting of a laser modulated by means of a rotating half-wave plate (OAM module, TA

Received: January 25, 2011
Revised: March 4, 2011
Published: March 18, 2011

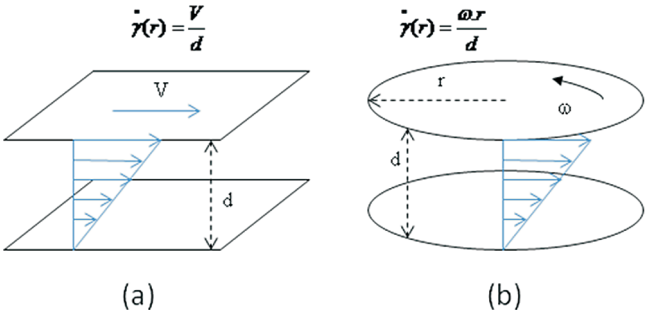

Figure 1. Schematic representation of the flow geometries: rectilinear (a) and torsional (b).

Instruments) and at the other side of the shear cell, a circular analyzer and a photodetector. The intensity measured by the detector is given by

$$I \approx I_0[1 + \sin(4\Omega t + 2\varphi)\sin\delta] \quad (2)$$

where I_0 is the initial intensity, Ω is the angular speed of the rotating half-wave plate, and φ is the phase angle. The signal is analyzed using a decomposition of the form

$$I = I_{DC} + I_{sin}\sin(4\Omega t) + I_{cos}\cos(4\Omega t) \quad (3)$$

with I_{sin} and I_{cos} the amplitudes of the sine and cosine component in the signal.

The birefringence, $\Delta n'$, is then calculated as

$$\Delta n' = \frac{\lambda\delta'}{2\pi d} \quad (4)$$

where λ is the laser light wavelength (670 nm), d is the sample thickness, and δ' is the optical retardation calculated as

$$|\sin\delta'| = \frac{\sqrt{I_{sin}^2 + I_{cos}^2}}{I_{DC}} \quad (5)$$

In the sliding plate configuration, as described elsewhere,[10] the sample is sheared between two parallel glass plates that are incorporated in sample holders placed in oppositely moving conditioning blocks. Apertures are provided in the equipment to allow the transition of a laser beam through the sample in order to probe the structure in the flow−vorticity plane.

The setup allows achieving deformations up to a few hundred shear units, which is in the order of the shear rates realized in the outer layers of injection molded products. The unit is sufficiently rigid to withstand the normal forces generated during shear, even in case of highly viscous polymers.

The sliding plate concept ensures a constant shear rate throughout the sample. After crystallization, the sample thickness is typically between 50 and 100 μm (in this study: about 70 μm). For the samples under consideration in this work, it has been checked that no transcrystallization due to the glass surfaces was present.

The crystallization protocol consists of an annealing step at 200 °C to erase the thermomechanical history of the material. Next, the sample is cooled to different crystallization temperatures between 98 and 120 °C at a cooling rate of about 10 °C/min. When the crystallization temperature is reached, a shear pulse is applied in which shear rate and shearing time can be varied independently.

Despite the fact that the flow cell produces a homogeneous shear across the sample, the use of this cell in the determination of the threshold conditions for structural orientation is not straightforward. The method merely provides a single point measurement with only one set of shear rate and shear time. Hence, in order to accurately define the onset of orientation, many experiments need to be performed. In this respect, a combinatorial approach employing a torsional parallel disk geometry is more efficient. A wide range of shear rates is experienced by a polymer sample in this geometry. Hence, a single experiment significantly reduces the number of experiments required for the detection of the threshold conditions. While the homogeneous flow produced by the sliding plate geometry needs only one point to track structural evolutions of a polymer during shear, the torsional geometry, producing a wide range of radially distributed shear rates, requires access to many points across the sample which makes this geometry problematic to be used for online measurements. Thus, contrary to a simple realization of online measurements in a sliding plate geometry, the torsional geometry technique is based on offline measurements. After imposing a temperature−shear protocol, the samples are allowed to fully crystallize after which they are recuperated for further analysis. This second setup is realized using a Linkam shear cell device (CSS-450) modified to deal with highly viscous samples.[3] Unloading the sample is crucial in this respect since one wants to recuperate samples without breaking them. The sample thickness was set to d = 0.5 mm, which made the crystallized samples rigid enough to maintain their shape at unloading from the shear device while also keeping samples transparent for subsequent SAXS experiments to analyze the structural morphology of the recuperated samples.

The temperature−shear protocol of the second setup is similar to the protocol used with the first setup. It consist of an annealing step at high temperature for 5 min followed by cooling at a rate of about 10 °C/min to a range of temperatures at which a shear pulse is applied (98, 112, 115, and 120 °C). The sample was kept at the temperature of shearing for another 20 min and cooled down to 90 °C at a rate of 1 °C/min and then to room temperature at a rate of 20 °C/min to complete the crystallization. When the temperature of shearing is reached, a shear pulse is applied in which angular speed of the rotating disk, ω, and shearing time can be varied independently. Shear rates from 0 to 200 s^{-1} have been explored in this study with the maximum value controlled via ω in each experiment: $\dot{\gamma}_{max} = \omega r/d$ (Figure 1b). The shear pulse duration did not exceed 12 s in the presented experiments; however, in contrast to the rectilinear geometry, the torsional geometry does not impose constrains on t_s.

The samples recuperated from both geometries have been analyzed by SAXS (Bruker AXS NanoSTAR, Cu Kα radiation, equipped with a HiStar area detector and a semitransparant beamstop). The instrument was set to camera length 1.05 m, which allowed patterns corresponding to scattering vectors 0.01 $Å^{-1} < q < 0.2$ $Å^{-1}$ to be recorded ($q = 4\pi\sin\theta/\lambda$, where θ is a half of scattering angle and λ = 1.54 Å is the X-ray wavelength). The samples from the rectilinear geometry have been scanned across the length of the sample parallel to the flow direction and the samples from the torsional geometry across the diameter of the sample. The obtained two-dimensional scattering

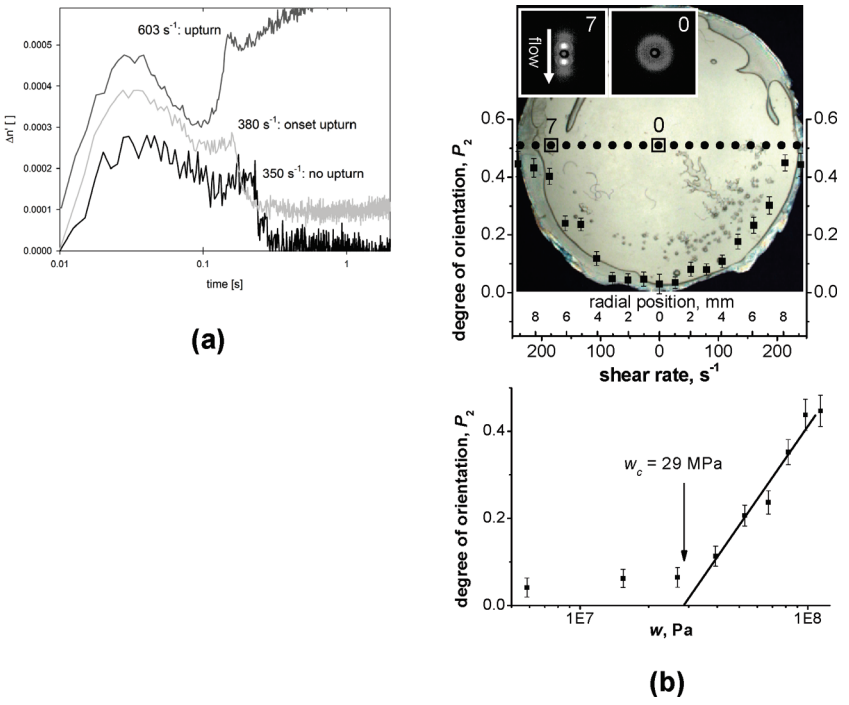

Figure 2. (a) Typical birefringence curves for crystallization experiments at 103 °C (strain = 100 performed in sliding plate geometry). (b) Degree of orientation across the samples after shear-induced crystallization measured by small-angle X-ray scattering (SAXS) for the torsional parallel plates geometry, ω = 13.33 rad/s and t_s = 6 s at 120 °C. The dotted line across the image of the sample indicates points of the SAXS scan. The insets show representative SAXS patterns with the sides corresponding to q = 0.067 Å^{-1} (numbers indicate position of the pattern in the scan in millimeters). The bottom graph represents a linear−log plot of the degree of orientation of the torsional geometry sample versus specific work, w.

patterns have been azimuthally integrated (q range from 0.01 to 0.05 Å^{-1}), and the resulting intensity profiles, $I(\phi)$, have been used to calculate the degree of orientation of lamellar structure after the shear-induced crystallization experiments, expressed via the Herman's orientation function P_2 defined as

$$P_2 = \frac{3\langle \cos^2 \varphi \rangle - 1}{2} \tag{6}$$

where

$$\langle \cos^2 \varphi \rangle = \frac{\int_0^{\pi/2} I(\varphi) \cos^2 \varphi \sin \varphi \, d\varphi}{\int_0^{\pi/2} I(\varphi) \sin \varphi \, d\varphi} \tag{7}$$

is the average angle of the lamella normal with a chosen direction which is taken to be the flow direction.

In order to calculate the specific work (eq 1), the viscosity is needed. Hereto, linear viscoelastic measurements have been performed using an Ares rheometer (TA Instruments). The time−temperature superposition method has been used to extend the range of frequencies or, by using the Cox−Merz rule, the shear rates. In order to further increase the shear rate window, a Cross model was fitted through the data that allowed to extrapolate viscosity values to high shear rates. The obtained temperature coefficient a_T has been used to calculate the viscosity at the crystallization temperature, needed to calculate the specific work.

RESULTS AND DISCUSSION

In this section, the two experimental setups will be used to explore the onset of oriented morphology formation. A typical example of results obtained by the sliding plate setup is demonstrated in Figure 2a. In order to detect the onset of orientation, the birefringence during flow provides useful information. For instance, when a shear rate of 350 s^{-1} is applied, the birefringence first increases due to the induced molecular orientation, after which a steady-state birefringence is reached. When shear is removed, the birefringence fully relaxes. When the shear rate is increased, for instance 380 s^{-1}, the birefringence exhibits an upturn at the end of the shear step. The evolution of the birefringence with increasing shear rate has also been observed by Kumaraswamy et al.[11] and Seki et al.[12] during their extrusion die experiments (constant wall shear stress, varying shear time) and by Langouche[10] and Baert et al.[8] in experiments with the same shear cell (constant strain, varying shear rate). Kumaraswamy et al.[11] demonstrated by means of wide-angle X-ray diffraction experiments that this upturn indicates the presence of long-lived oriented structures, which form the template for subsequent oriented crystal growth, more in particular for shish-kebab structures. Hence, the appearance of such an upturn in the birefringence can be used to define the onset of shish-kebab dominated structures. The shear parameters used for this experiment can then be used to calculate the critical specific work as specified by eq 1. When shear rate is even more increased (e.g., 603 s^{-1} in Figure 2), this upturn is prominently present. When flow is removed, crystallization sets in immediately.

In the torsional geometry, every radial point of the sample is associated with a particular shear rate and hence also associated

dx.doi.org/10.1021/ma200165q |Macromolecules 2011, 44, 1783–1787

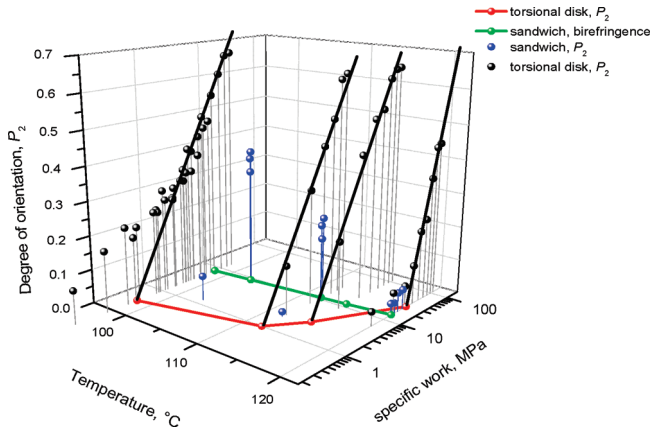

Figure 3. A combined 3-dimensional representation of shear-induced crystallization results obtained for sandwich and torsional geometries including temperature of shearing, degree of orientation, and specific work required for the onset of oriented morphology.

with a certain amount of work applied to the polymer (see Figure 2b). The specific work experienced by the polymer during flow can be calculated for each point using eq 1 in which the shear rate is based on the radial distribution of shear rates across the sample (Figure 1b). In addition, SAXS measurements of the degree of orientation (P_2) are used to detect the threshold conditions for the formation of oriented structures. It has been shown before[4] that the degree of orientation plotted versus the specific work essentially collapses onto a master curve. An example of this approach is given in Figure 2b. Here the dotted lines indicate the locations at which SAXS profiles have been obtained. From this plot, it can be seen that the degree of orientation drastically increases above a certain threshold value which is defined to be the critical work. A logarithmic function has been used in this work to find intersect with the axis of specific work (x-axis) to obtain w_c $\{P_2(w) = a + b \ln(w)$, where a and b are fitting parameters and $w_c = \exp(-a/b)\}$. The degree of orientation detected by SAXS changes in a relatively narrow interval (less than 1 order of magnitude) and does not provide enough data to justify either this function should be of another kind. The logarithmic function appears as a line in a plot of a linear−log format (Figure 2b).

Figure 3 shows the values of the degree of orientation, expressed by P_2, as a function of the specific work and as a function of temperature (98, 112, 115, and 120 °C). As is clear from the plot, the degree of orientation drastically increases above a certain critical value for all temperatures investigated. A noticeable deviation from the line is observed for the results obtained at 98 °C. This effect has been reported for other polymers and can occur at temperatures below the melting point of spherulites.[4] The temperature-driven formation of spherulitic nuclei, which are likely to appear below 111 °C in any zone of the poly(1-butene) sample, are deformed by the flow resulting in an elongated spherulite morphology. Thus, the anisotropy caused by this spherulitic morphology also contributes to the degree of orientation, which is detectable at $w < w_c$ when no shear-induced nucleation occurs.

Both methods give a value of the critical work required to obtain oriented structures, and both methods demonstrate an increase of the specific work with temperature (Figure 3, temperature-specific work plane). However, the absolute values of the critical work are different. The differences can be put in perspective of a recent model proposed by Mykhaylyk et al. to describe the formation of oriented structure.[4,13] In that model, the crucial point is the formation of shish nuclei that are above a critical size. In our experiments, the curve obtained from off-line measurements, SAXS experiments (Figure 3, red curve), yields threshold conditions for the formation of stable shish nuclei since SAXS directly measures the final orientation in the crystallized sample. This curve corresponds to the moment when the aggregation of stretched molecules (shish precursors) is above the critical size required for the formation of stable nuclei at the thermodynamic conditions of shearing used. Hence, after cessation of shear, the formed aggregates—shish nuclei—remain stable and participate as crystal nuclei for the remainder of the crystallization process, causing growth of crystals into oriented kebabs. The curve obtained with the online birefringence technique (Figure 3, green line) yields threshold conditions for the occurrence of an upturn in birefringence during flow. The curve indicates the moment at which birefringence becomes sensitive enough to identify structural birefringence—on top of the birefringence coming from oriented molecules—originating from aggregates of stretched molecules. If the concentration of aggregates formed during flow is high enough, the upturn is observed, but it does not necessarily mean that the aggregates have reached the critical size of stable nuclei at the thermodynamic conditions of the shear experiment. Two scenarios can be considered in this case: the critical specific work required for the formation of shish nuclei is either below (scenario 1) or above (scenario 2) the specific work creating the aggregates detectable by birefringence. Thus, the birefringence measurements should lead to either overestimation (scenario 1) or underestimation (scenario 2) of w_c.

Comparing the two methods, we can conclude that at low temperatures the upturn in birefringence is happening when the specific work is higher than the amount of work required for the formation of stable shish nuclei (scenario 1). At 120 °C, however, an opposite situation is seen (scenario 2): the concentration of aggregates is high enough to cause an upturn in the birefringence signal, but the corresponding specific work is below the amount of work required for the formation of stable shish nuclei (i.e., the size of the aggregates is below the critical size for a stable nucleus) at this temperature. Hence, after cessation of flow, all aggregates created by flow melt down as their size is below the critical size. The latter is supported by the fact that at 120 °C the birefringence relaxes completely when flow is stopped.

In order to further support these observations, an offline SAXS analysis has been performed on samples processed in the sandwich cell at different flow conditions corresponding to both the upturn in birefringence and the moment of shish nuclei formation detected by torsional geometry. A representative set of SAXS patterns for the samples demonstrating the upturn in birefringence display a very strong orientation at 103 and 112 °C (Figure 4). These SAXS data suggest that the onset to oriented structures has already occurred well below the value detected by the online birefringence method. On the other hand, samples recuperated after shearing at 120 °C virtually show no orientation, indicating that more work is needed in order to cross the boundary toward the shish nuclei formation. SAXS patterns of the samples sheared by sliding geometry at threshold conditions of shish nuclei formation have shown virtually no orientation reproducing the results obtained by torsional geometry. A combined 3D plot of the degree of orientation of samples originating from both geometries demonstrates a quantitative

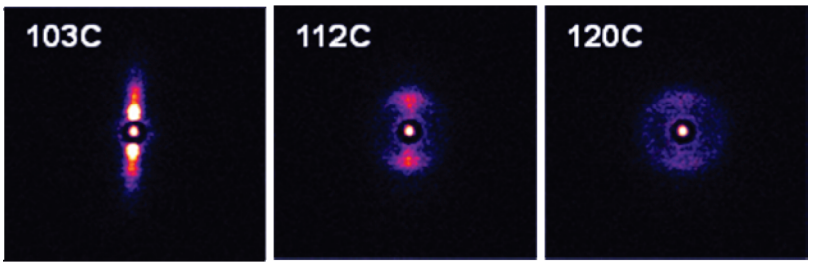

Figure 4. Representative set of SAXS patterns of samples recuperated from the sandwich cell after shear-induced crystallization ($\dot{\gamma}$ = 411 s^{-1}, γ = 96 at 103 °C; $\dot{\gamma}$ = 261 s^{-1}, γ = 145 at 112 °C; $\dot{\gamma}$ = 603 s^{-1}, γ = 164 at 120 °C). The direction of shear is vertical. The sides of the patterns scale to 0.17 $Å^{-1}$.

correlation of the results (Figure 3). All the obtained points virtually belong to the same surface representing the degree of orientation. This suggests that the shear-induced structural morphology is entirely controlled by flow conditions and is independent of shear geometry.

While structural morphology is reproducible by both geometries at similar flow conditions, there is no direct correlation between the critical specific works obtained by either online birefringence measurements or offline SAXS measurements. The apparent discrepancy is based on the fact that the measured magnitudes correspond to different phenomena taking place in polymer during shear-induced crystallization. The comparison shows that the birefringence technique has limited application and can be sensitive to the formation of shish nuclei only at certain circumstances, when the critical work required for the formation of high concentration of shish precursors, detectable by birefringence, is below the threshold conditions required for the formation of stable shish nuclei. In the considered examples it is observed at temperatures around 120 °C and above.

CONCLUSIONS

The results show that both sliding plates and torsional disks geometries produce similar morphologies at the same flow conditions. The application of torsional geometry covering a wide range of shear rates in a single experiment can be effective at the first stage to detect the threshold conditions for the formation of shish nuclei and the onset of oriented morphology. When precise measurements of the flow conditions would be required, the sliding plate geometry would be a preferable technique to use. The application of this geometry is time-consuming, but it enables a secondary flow to be avoided in the measurements. The birefringence technique is an effective tool for online measurements of structural evolution of semicrystalline polymers; however, an application of this technique is restricted by its sensitivity, and the onset of oriented morphology can be detected only at limited conditions. It is possible to suggest that birefringence measurements, coupled with off-line SAXS measurements, can be calibrated and adjusted to track the evolution of structural morphology online.

AUTHOR INFORMATION

Corresponding Author

*E-mail: O.Mykhaylyk@sheffield.ac.uk (O.O.M.); peter.vanpuyvelde@cit.kuleuven.be (P.V.P.).

ACKNOWLEDGMENT

M.D. and P.V.P. are indebted to the Onderzoeksfonds K.U. Leuven (GOA 02/009) for their financial support.

REFERENCES

(1) Kumuraswamy, G. *J. Macromol. Sci., Polym. Rev.* **2005**, *C45*, 375–397.
(2) Keller, A. *Rep. Prog. Phys.* **1968**, *31*, 623–704.
(3) Mykhaylyk, O. O.; Chambon, P.; Graham, R. S.; Fairclough, P. A.; Olmsted, P. D.; Ryan, A. J. *Macromolecules* **2008**, *41*, 1901–1904.
(4) Mykhaylyk, O. O.; Chambon, P.; Impradice, C.; Fairclough, J. P. A.; Terrill, N. J.; Ryan, A. J. *Macromolecules* **2010**, *43*, 2389–2405.
(5) Baert, J.; Langouche, F.; Van Puyvelde, P. *Fibres Text. East. Eur.* **2008**, *16*, 73–76.
(6) Housmans, J. W.; Steenbakkers, R. J. A.; Roozemond, P. C.; Peters, G. W. M.; Meijer, H. E. H. *Macromolecules* **2009**, *42*, 5728–5740.
(7) Janeschitz-Kriegl, H.; Ratajski, E.; Stadlbauer, M. *Rheol. Acta* **2003**, *42*, 355–364.
(8) Baert, J.; Van Puyvelde, P.; Langouche, F. *Macromolecules* **2006**, *39*, 9215–9222.
(9) Yamashita, M.; Kato, M. *J. Appl. Crystallogr.* **2007**, *40*, s650–s655.
(10) Langouche, F. *Macromolecules* **2006**, *39*, 2568–2573.
(11) Kumaraswamy, G.; Issaian, A. M.; Kornfield, J. K. *Macromolecules* **1999**, *32*, 7537–7547.
(12) Seki, M.; Thurman, D. W.; Oberhauser, J. P.; Kornfield, J. K. *Macromolecules* **2002**, *35*, 2583–2594.
(13) Mykhaylyk, O. O.; Fernyhough, C. M.; Okura, M.; Fairclough, J. P. A.; Ryan, A. J.; Graham, R. *Eur. Polym. J.* **2010**, 10.1016/j.eurpolymj.2010.09.021.